

Synthesis and Characterization of Superparamagnetic Fe₃O₄@SiO₂ Core-Shell Composite Nanoparticles

Meizhen Gao, Wen Li, Jingwei Dong, Zhirong Zhang, Bingjun Yang

Key Lab for Magnetism and Magnetic Materials of MOE, Lanzhou University, Lanzhou, China.
Email: liwen3311@126.com

Received January 9th, 2011; revised March 8th, 2011; accepted March 15th, 2011.

ABSTRACT

The Fe₃O₄@SiO₂ composite nanoparticles were obtained from as-synthesized magnetite (Fe₃O₄) nanoparticles through the modified Stöber method. Then, the Fe₃O₄ nanoparticles and Fe₃O₄@SiO₂ composite nanoparticles were characterized by means of X-ray diffraction (XRD), Raman spectra, scanning electron microscope (SEM) and vibrating sample magnetometer (VSM). Recently, the studies focus on how to improve the dispersion of composite particle and achieve good magnetic performance. Hence effects of the volume ratio of tetraethyl orthosilicate (TEOS) and magnetite colloid on the structural, morphological and magnetic properties of the composite nanoparticles were systematically investigated. The results revealed that the Fe₃O₄@SiO₂ had better thermal stability and dispersion than the magnetite nanoparticles. Furthermore, the particle size and magnetic property of the Fe₃O₄@SiO₂ composite nanoparticles can be adjusted by changing the volume ratio of TEOS and magnetite colloid.

Keywords: Magnetite Nanoparticles, Fe₃O₄@SiO₂ Composite Nanoparticles, Dispersion, Thermal Stability, Particle Size, Magnetic Property

1. Introduction

Magnetite nanoparticles have attracted a great deal of attention because of their unique physicochemical properties and great potential use in various biomedical applications, such as contrast agents in magnetic resonance imaging (MRI), carriers for targeted drug delivery, the magnetic separation in microbiology, biochemical sensing [1-4], etc.

However, the magnetite nanoparticles are unstable in air and easily agglomerated after synthesis. The surface coatings and functionalization could effectively solve these problems [5-9]. Silica surfaces are chemically stable, biocompatible and can be easily functionalized for bioconjugation purpose. Hence silica-coated magnetite composite nanoparticles (Fe₃O₄@SiO₂/core-shell) have been synthesized by many groups [10-12]. Recently, silica coated magnetite functionalized with γ -mercaptopropyltrimethoxysilane have been successfully applied to extract Cd²⁺, Cu²⁺, Hg²⁺, and Pb²⁺ from water in a wide pH range [13].

In this work, the silica-coated magnetite nanoparticles are synthesized through two steps. The magnetite nanoparticles are firstly prepared by coprecipitation method [5]. Then the magnetite nanoparticles are used to synthesize the Fe₃O₄@SiO₂ composite nanoparticles through the modified Stöber method [12]. The thermal stability and morphologies of Fe₃O₄ and Fe₃O₄@SiO₂ are studied. Afterward, the effects of experimental parameters, such as the volume of TEOS and magnetite colloid on the properties of Fe₃O₄@SiO₂ composite nanoparticles are also systematically investigated.

2. Experiment

2.1. Materials

The iron (II) chloride tetrahydrate (FeCl₂·4H₂O, 99.7%), iron (III) chloride hexahydrate (FeCl₃·6H₂O, 99.0%), hydrochloric acid (HCl, 35 wt.% - 37 wt.%), sodium hydroxide (NaOH, 96 %), polyethylene glycol (PEG, Mw=2000), tetraethyl orthosilicate (TEOS, 28%), ammonia (NH₃·H₂O, 25 wt.% - 28 wt.%), and ethanol (C₂H₅OH, 99.7%) are all commercially available. Distilled water is

also used for preparation of the solutions.

2.2. Preparations of the Magnetite Nanoparticles

An aqueous solution of Fe ions with a molar ratio of Fe(II)/Fe(III) \sim 0.5 was prepared by dissolving 5.46 g FeCl₃·6H₂O, 2.00 g FeCl₂·4H₂O and 0.6 g PEG-2000 in 60 ml of aqueous acid of 50 ml distilled water with 10 ml of 1 M HCl, and then added dropwise into 100 ml of 1 M NaOH with 1.0 g PEG-2000 solution under vigorous stirring at 60°C. The reaction was carried out in an inert atmosphere by purging the reactor with high purity argon (99.9%) all through. After all of the Fe ions solution was added, the mixture was stirred for a further 2 h. Then the colloid solution was washed by distilled water for several times until it is neutral. A part of colloid is dried in fridge. The remnant of the colloid was dispersed in distilled water by ultrasonic, and then was ready for coating process.

2.3. Preparations of the Fe₃O₄@SiO₂ Composite Nanoparticles

Placed a certain volume of Fe₃O₄ colloid (2 wt.%) and distilled water (total volume is 19 ml) into a 250 ml three-neck flask, then added 80 ml ethanol, a certain amount of TEOS and ammonia under vigorous stirring (800 rpm) at room temperature for 12 h. The obtained Fe₃O₄@SiO₂ colloid was washed by repeated cycles of distilled water and ethanol. Then, the final products were dried in an oven at 60°C for 24 h.

2.4. Characterization

The phase identification and crystalline structures of the nanoparticles was characterized by X-ray powder diffraction of the dried samples using a D/Max-2400 X-ray diffractometer equipped with a Cu K α monochromatic radiation source ($\lambda = 1.54187 \text{ \AA}$). The Raman spectra of nanoparticles were collected using a Laser Confocal Raman Spectroscopy (LCRS). The morphologies were observed using a scanning electron microscope Hitachi S4800 operating at an accelerating voltage of 15 kV. Magnetic measurements were performed using a vibrating sample magnetometer Lake Shore 7304.

3. Result and Discussion

3.1. Thermal Stability of Fe₃O₄ Nanoparticles and Fe₃O₄@SiO₂ Composite Nanoparticles

Phase identification is one of the most important uses of XRD. Firstly, we obtained XRD pattern of the materials, then, we compare data with known standards in the JCPDS file to preliminary identify the materials.

As shown in **Figure 1**, XRD patterns of Fe₃O₄ after heat treatments are shown. For the nanoparticles without (**Figure 1(a)**) and with heat treatment at 200°C (**Figure**

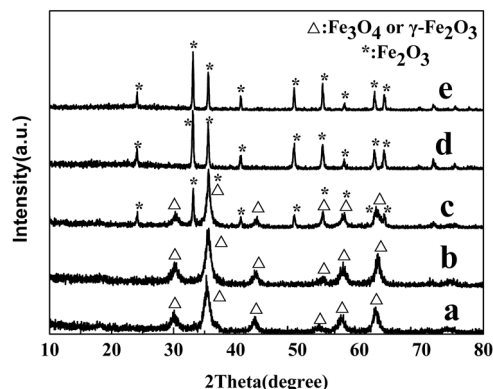


Figure 1. XRD patterns of Fe₃O₄ a nanoparticles under different temperature heat treatments for 3 h. (a: without treatment; b: 200°C; c: 400°C; d: 600°C; e: 800°C).

1(b)); 400°C (**Figure 1(c)**), the XRD patterns (marked Δ) are well indexed to the cubic spinel phase of magnetite (JCPDS No. 89-43191). No other significant peaks can be observed in **Figures 1(a)** and **(b)**, however, because the diffraction peaks of γ -Fe₂O₃ are similar with Fe₃O₄, we can only confirm that the nanoparticles with and without 200°C heat treatment do not contain impurities except γ -Fe₂O₃. A further investigation will be obtained by Raman. What's more, the characteristic peaks of spinel structure Fe₂O₃ (Marked *) can be simultaneously observed in **Figure 1(c)**. We can infer that Fe₃O₄ can be completely transformed into Fe₂O₃ when Fe₃O₄ experiences a heat treatment at 400°C for enough time. Upon heating at 600°C for 3 h (**Figure 1(d)**), all of Fe₃O₄ nanoparticles transform into Fe₂O₃.

Similarly, Raman spectra are also used to identify the phase of materials. To verify whether there is a phase transition from Fe₃O₄ to γ -Fe₂O₃ for the nanoparticles with and without 200°C heat treatment, the corresponding Raman spectra were also obtained. **Figure 2** illustrates the Raman spectra of magnetite nanoparticles before (**Figure 2(a)**) and after (**Figure 2(b)**) heat treatment at 200°C. As we can see the peaks at 350 cm⁻¹, 550 cm⁻¹ and 670 cm⁻¹ can be observed (**Figure 2(a)**), which can be attributed to T_{2g,3}, T_{2g,2}, A_{1g} vibration mode of Fe₃O₄ respectively. At higher wavenumber (\sim 1378 cm⁻¹), there are no apparent peak. Hence, this result gives the obvious evidence for the existence of Fe₃O₄ other than γ -Fe₂O₃ [14].

In **Figure 2(b)**, the peak at 1400 cm⁻¹ as well as peaks at 350 cm⁻¹, 550 cm⁻¹ and 670 cm⁻¹ indicates part of Fe₃O₄ transforms into γ -Fe₂O₃. We can confirm Fe₃O₄ will completely transform into γ -Fe₂O₃ under a 200°C heat treatment for a long enough time.

In general, the Fe₃O₄ nanoparticles will partly transform into γ -Fe₂O₃ under a 200°C heat treatment for 3 h. On experiencing a 600°C heat treatment for 3 h, the

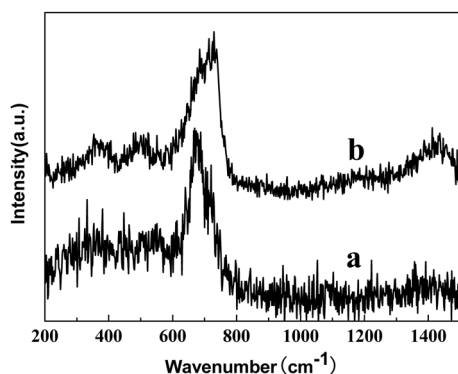


Figure 2. Raman spectra of Fe₃O₄ nanoparticles before (a); and after heat treatment at 200°C for 3 h (b).

Fe₃O₄ nanoparticles will completely transform into Fe₂O₃.

Thermal stability of Fe₃O₄@SiO₂ composite nanoparticles is also investigated. In **Figure 3**, XRD patterns of Fe₃O₄@SiO₂ after heat treatments are shown. The peaks of Fe₃O₄ and SiO₂ amorphous hump at 23° can be observed for all samples. In addition, characteristic peaks of Fe₂O₃ appear (Marked *) with the heat treatment temperature of 800°C (**Figure 3(e)**). After 800°C heat treatment for 3 h, the predominant phase of the Fe₃O₄@SiO₂ composite nanoparticles is still Fe₃O₄ (**Figure 3(e)**). But the pure Fe₃O₄ has completely transformed into Fe₂O₃ at 600°C for 3 h (see **Figure 1(d)**). This suggests that the Fe₃O₄@SiO₂ has a significantly higher thermal stability than the pure Fe₃O₄.

3.2. The improvement in Dispersion by SiO₂ Coating

The morphological characteristics of the Fe₃O₄ nanoparticles and Fe₃O₄@SiO₂ composite nanoparticle are shown in **Figure 4**. The Fe₃O₄ nanoparticles are agglomerated seriously and the size is very small (**Figure 4(a)**). But the composite nanoparticles are almost monodisperse with uniform size (**Figure 4(b)**). It proves the dispersion of Fe₃O₄@SiO₂ composite nanoparticles is apparently improved.

3.3. The effect of the Volume of TEOS on the Structural, the Morphological and the Magnetic Properties

While increased the volume ratio of TEOS, other conditions, such as 4 ml Fe₃O₄ colloid, 2 ml ammonia at room temperature, kept the same.

Figure 5 summarizes the crystalline structure dependence on the ratio of TEOS. The amorphous hump of SiO₂ around 23° and the characteristic peaks of Fe₃O₄ around 35.4° can be observed for all samples. The increase in intensity of amorphous hump suggests that SiO₂

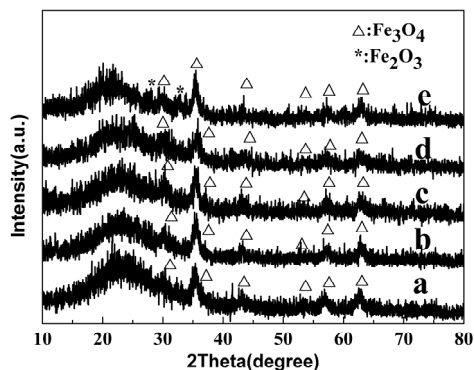


Figure 3. XRD patterns of Fe₃O₄@SiO₂ nanoparticles under different temperature heat treatments for 3 h. (a: without treatment; b: 200°C; c: 400°C; d: 600°C; e: 800°C).

content accumulates with the TEOS volume increasing.

Figure 6, the SEM images of Fe₃O₄@SiO₂ composite nanoparticles with different ratio of TEOS, indicates that the increasing TEOS volume ratio leads to a bigger size of composite particle. This can be ascribed to the fact that when the dosage of TEOS increases, the quantity of SiO₂ increases. Therefore, the Fe₃O₄ particles are adequately coated, and the size of composite nanoparticles increases with ratio of TEOS increasing. This result consisted with the XRD result.

Room temperature magnetic properties of Fe₃O₄@SiO₂ composite nanoparticles with different ratio of TEOS were measured using VSM, as shown in **Figure 7**.

It is manifest in **Figure 7** that there is no hysteresis in the magnetization curve, the coercivity field and remnant magnetization cannot be found from the curve. It confirms that Fe₃O₄@SiO₂ composite nanoparticles are superparamagnetic. The magnetization does not saturate at 11000 Oe, and the values are 12.7 emu/g, 6.3 emu/g, 4.3 emu/g, 3.1 emu/g and 2.4 emu/g for various TEOS concentrations respectively, which shows a trend of gradual decrease. The reason is that SiO₂ coating grows thicker with increasing concentration of TEOS, thus reduces their magnetism. In a word, the magnetism of the composite particles can be controlled by adjusting the concentration of TEOS.

3.4. The Effect of the Volume of Magnetite Colloid on the Structural, the Morphological and the Magnetic Properties

The influence of the concentration of magnetite colloid on structure, morphology and magnetism were also studied here. During this reaction, the ammonia and TEOS both were fixed to 2 ml, while the volume of magnetite colloid was different.

Figure 8 shows XRD spectra of Fe₃O₄@SiO₂ composite nanoparticles with different ratio of magnetite

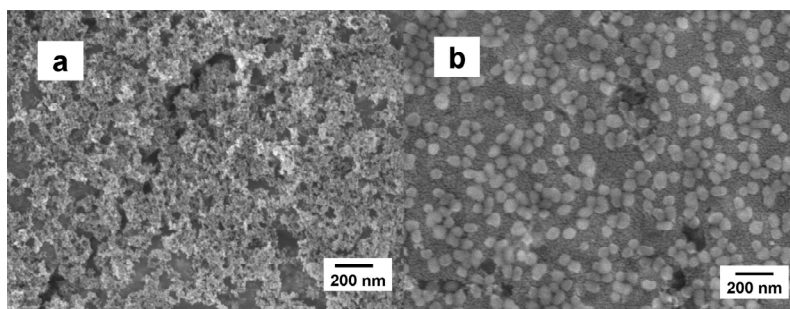


Figure 4. SEM images of Fe_3O_4 nanoparticles (a) and $\text{Fe}_3\text{O}_4@\text{SiO}_2$ composite nanoparticles (b).

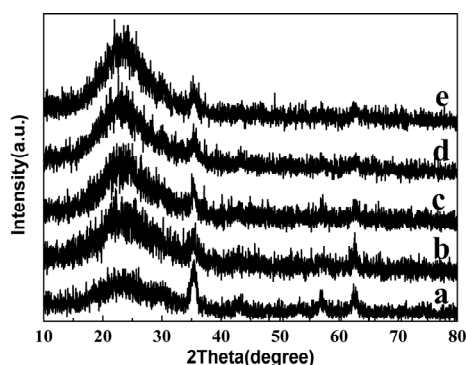


Figure 5. XRD patterns of $\text{Fe}_3\text{O}_4@\text{SiO}_2$ nanoparticles synthesized with different TEOS volume (a: 1 ml TEOS; b: 2 ml TEOS; c: 3 ml TEOS; d: 5 ml TEOS; e: 8 ml TEOS).

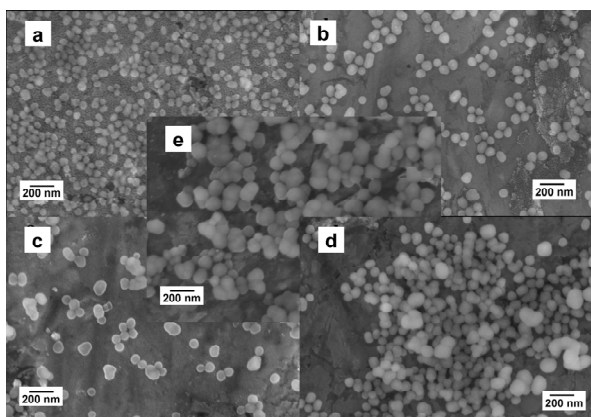


Figure 6. SEM images of $\text{Fe}_3\text{O}_4@\text{SiO}_2$ nanoparticles synthesized at different TEOS volume (a: 1 ml TEOS; b: 2 ml TEOS; c: 3 ml TEOS; d: 5 ml TEOS; e: 8 ml TEOS).

colloid. The amorphous hump of SiO_2 and characteristic peaks of Fe_3O_4 can be observed for all samples. But the width and the intensity of the amorphous hump decreases, opposing to the increasing volume of Fe_3O_4 colloid.

As we can see the morphologies of $\text{Fe}_3\text{O}_4@\text{SiO}_2$ composite nanoparticles with different ratio of TEOS in **Figure 9**, the size of composite nanoparticles tends to reduce gradually and the dispersion becomes worse with in-

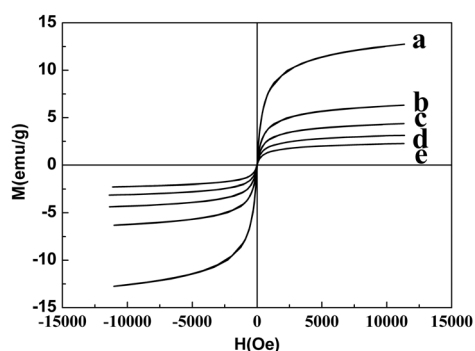


Figure 7. Magnetic hysteresis curves of $\text{Fe}_3\text{O}_4@\text{SiO}_2$ nanoparticles synthesized at different TEOS volume (a: 1 ml TEOS; b: 2 ml TEOS; c: 3 ml TEOS; d: 5 ml TEOS; e: 8 ml TEOS).

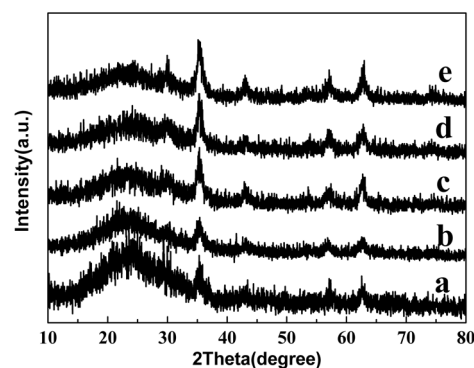


Figure 8. XRD pattern of $\text{Fe}_3\text{O}_4@\text{SiO}_2$ nanoparticles with different magnetite colloid volume (a: 1 ml magnetite colloid; b: 2 ml magnetite colloid; c: 4 ml magnetite colloid; d: 6 ml magnetite colloid; e: 8 ml magnetite colloid).

creasing amount of Fe_3O_4 colloid. The reason is just that for increasing quantity of Fe_3O_4 colloid, the concentration of the SiO_2 becomes diluted and consequently the SiO_2 is inadequate to coat Fe_3O_4 colloid. Therefore composite particles become agglomerated, accompanied by reduced size of theirs.

The magnetization curve of $\text{Fe}_3\text{O}_4@\text{SiO}_2$ nanoparticles with different volume of magnetite colloid are illustrated in **Figure 10**. It is also without hysteresis, and no sign of

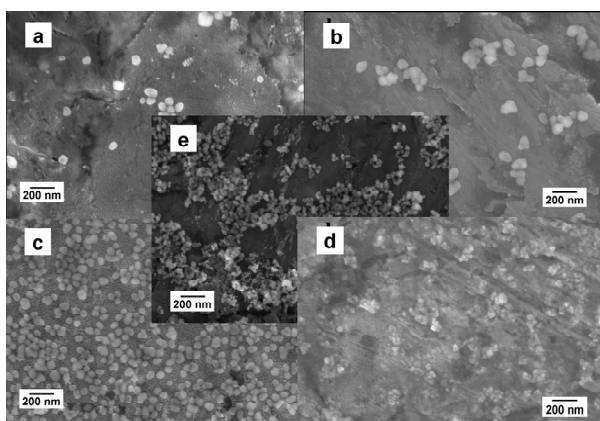


Figure 9. SEM images of Fe₃O₄@SiO₂ nanoparticles with different magnetite colloid volume (a: 1 ml magnetite colloid; b: 2 ml magnetite colloid; c: 4 ml magnetite colloid; d: 6 ml magnetite colloid; e: 8 ml magnetite colloid).

finite coercivity field and remnant magnetization can be found from the curve. From the magnetization curve, we can also see that the magnetization does not saturate at 11000 Oe magnetic fields. The magnetization is 5.2 emu/g, 8.3 emu/g, 16.7 emu/g, 20.2 emu/g and 23.8 emu/g for increasing volume of colloid. The results are well coincident with XRD spectrum and SEM results. This highlights proper concentration of magnetite colloid redounds to good dispersion and magnetism.

4. Conclusions

In summary, the Fe₃O₄ nanoparticles are seriously agglomerated after synthesis. Additionally, the Fe₃O₄ nanoparticles completely transform into Fe₂O₃ after a 600 °C heat treatment for 3 h.

What's more, the Fe₃O₄@SiO₂ composite nanoparticles are almost monodisperse. It proves the SiO₂ coating remarkably improves the dispersion of Fe₃O₄ nanoparticles. When Fe₃O₄@SiO₂ composite particles experience an 800 °C heat treatment for 3 h, the major phase is still Fe₃O₄, which verifies that the composite particles exhibit better thermal stability than magnetite nanoparticles. Besides, silica surfaces are chemically stable, biocompatible and can be easily functionalized for bioconjugation purposes, Fe₃O₄@SiO₂ composite nanoparticles have great potential applications in various biomedical fields, such as DNA purification, protein-separation, targeted drug delivery, magnetic hyperthermia and magnetofection. In modified Stöber method, the experimental parameters such as volumes of TEOS and magnetite colloid are discussed. The particle size, dispersion and magnetic properties of the Fe₃O₄@SiO₂ composite particles can be controlled by changing the volume of TEOS and the magnetite colloid.

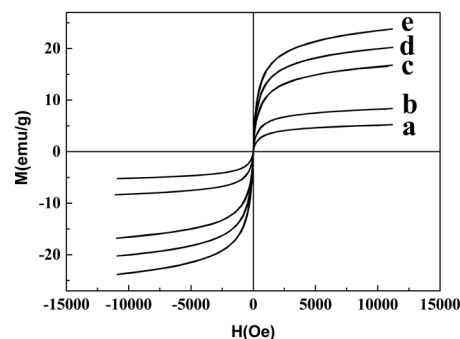


Figure 10. Magnetic hysteresis curves of Fe₃O₄@SiO₂ nanoparticles with different magnetite colloid volume (a: 1 ml magnetite colloid; b: 2 ml magnetite colloid; c: 4 ml magnetite colloid; d: 6 ml magnetite colloid; e: 8 ml magnetite colloid).

5. Acknowledgements

This work was financially supported by the Key grant Project of Chinese Ministry of Education (Grant No. 309027), and by the National Science Fund for Distinguished Young Scholars (Grant No. 50925103).

REFERENCES

- [1] C. Sun, J. S. H. Lee and M. Q. Zhang, "Magnetic Nanoparticles in MR Imaging and Drug Delivery," *Advanced Drug Delivery Reviews*, Vol. 60, No. 11, August 2008, pp. 1252-1265. doi:10.1016/j.addr.2008.03.018
- [2] A. K. Gupta and M. Gupta, "Synthesis and Surface Engineering of Iron Oxide Nanoparticles for Biomedical Applications," *Biomaterials*, Vol. 26, No. 18, June 2005, pp. 3995-4021. doi:10.1016/j.biomaterials.2004.10.012
- [3] R. Olsvik, T. Popovic, E. Skjerve, K. S. Cudjoe, E. Hornes, J. Ugelstad and M. Uhlen, "Magnetic Separation Techniques in Diagnostic Microbiology," *Clinical Microbiology Reviews*, Vol. 7, No. 1, January 1994, pp. 43-54.
- [4] M. N. Widjoatmodjo, A. C. Fluit, R. Torensma and J. Verhoef, "Comparison of Immunomagnetic Beads Coated with Protein A, Protein G, or Goat Anti-Mouse Immunoglobulins. Applications in Enzyme Immunoassays and Immunomagnetic Separations," *Journal of Immunological Methods*, Vol. 165, No. 1, 1993, pp. 11-19. doi:10.1016/0022-1759(93)90101-C
- [5] S. Y. Gan and M. Chow, "Carboxyl Group (-CO₂H) Functionalized Ferrimagnetic Iron Oxide Nanoparticles for Potential Bio-Applications," *Journal of Materials Chemistry*, Vol. 14, No. 18, 2004, pp. 2781-2786. doi:10.1039/b404964k
- [6] A. Kaushik, R. Khan, P. R. Solanki, P. Pandey, J. Alam, S. Ahmad and B. D. Malhotra, "Iron Oxide Nanoparticles—Chitosan Composite Based Glucose Biosensor," *Biosensors and Bioelectronics*, Vol. 24, No. 4, 2008, pp. 676-683. doi:10.1016/j.bios.2008.06.032

- [7] J. Sun, S. B. Zhou, P. Hou, Y. Yang, J. Weng, X. H. Li and M. Y. Li, "Synthesis and Characterization of Biocompatible Fe₃O₄ Nanoparticles," *Journal of Biomedical Materials Research*, Vol. 80A, No. 2, 2006, pp. 333-341.
- [8] M. D. Butterworth, L. Illum, S. S. Davis, "Preparation of Ultrafine Silica- and PEG-Coated Magnetite Particles," *Colloids and Surfaces A: Physicochemical and Engineering Aspects*, Vol. 179, No. 1, 2001, pp. 93-102. [doi:10.1016/S0927-7757\(00\)00633-6](https://doi.org/10.1016/S0927-7757(00)00633-6)
- [9] Q. Xu, X. J. Bian, L. L. Li, X. Y. Hu, M. Sun, D. Chen and Y. Wang, "Myoglobin Immobilized on Fe₃O₄@SiO₂ Magnetic Nanoparticles: Direct Electron Transfer, Enhanced Thermostability and Electroactivity," *Electrochemistry Communications*, Vol. 10, No. 7, 2008, pp. 995-999. [doi:10.1016/j.elecom.2007.12.002](https://doi.org/10.1016/j.elecom.2007.12.002)
- [10] T. Tago, T. Hatsuta, K. Miyajima, M. Kishida, S. Tashiro and K. Wakabayashi, "Novel Synthesis of Silica-Coated Ferrite Nanoparticles Prepared Using Water-in-Oil Microemulsion," *Journal of the American Ceramic Society*, Vol. 85, No. 9, 2002, pp. 2188-2194. [doi:10.1111/j.1151-2916.2002.tb00433.x](https://doi.org/10.1111/j.1151-2916.2002.tb00433.x)
- [11] A.-L. Morel, S. I. Nikitenko, K. Gionnet, A. Wattiaux, J. Lai-Kee-Him, C. Labrugere, B. Chevalier, G. Deleris, C. Petibois, A. Brisson and M. Simonoff, "Sonochemical Approach to the Synthesis of Fe₃O₄@SiO₂ Core-Shell Nanoparticles with Tunable Properties," *ACS NANO*, Vol. 5, No. 2, 2008, pp. 847-856. [doi:10.1021/mn800091q](https://doi.org/10.1021/mn800091q)
- [12] Z. I. Lei, Y. L. Li and X. Y. Wei, "A Facile Two-Step Modifying Process for Preparation of Poly (SSStNa)-Grafted Fe₃O₄/SiO₂ Particles," *Journal of Solid State Chemistry*, Vol. 181, No. 3, 2008, pp. 480-486. [doi:10.1016/j.jssc.2007.12.004](https://doi.org/10.1016/j.jssc.2007.12.004)
- [13] C. Z. Huang and B. Hu, "Silica-Coated Magnetic Nanoparticles Modified with Gamma-Mercaptopropyltrimethoxysilane for Fast and Selective Solid Phase Extraction of Trace Amounts of Cd, Cu, Hg, and Pb in Environmental and Biological Samples Prior to Their Determination by Inductively Coupled Plasma Mass Spectrometry," *Spectrochim Acta Part B: Atomic Spectroscopy*, Vol. 63, 2008, pp. 437-444.
- [14] D. L. A. De Faria, S. V. Silva, *et al.*, "Raman Microspectroscopy of Some Iron Oxides and Oxyhydroxides," *Journal of Raman Spectroscopy*, Vol. 28, No. 11, November 1997, pp. 873-878. [doi:10.1002/\(SICI\)1097-4555\(199711\)28:11<873::AID-JRS177>3.0.CO;2-B](https://doi.org/10.1002/(SICI)1097-4555(199711)28:11<873::AID-JRS177>3.0.CO;2-B)